# PCCP

## Accepted Manuscript

This article can be cited before page numbers have been issued, to do this please use: V. F. Korolovych, O. A. Grishina, O. Inozemtseva, A. V. Selifonov, D. N. Bratashov, S. G. Suchkov, L. A. Bulavin, O. E. Glukhova, G. Sukhorukov and D. A. Gorin, *Phys. Chem. Chem. Phys.*, 2015, DOI: 10.1039/C5CP05465F.




ROYAL SOCIETY OF CHEMISTRY

www.rsc.org/pccp

View Article Online
DOI: 10.1039/C5CP05465F
ROYAL SOCIETY OF CHEMISTRY

Journal Name

ARTICLE TYPE

Cite this: DOI: 10.1039/xxxxxxxxxx

# Impact of High-Frequency Ultrasound on Nanocomposite Microcapsules: *In Silico* and *In Situ* Visualization†

V.F. Korolovych,[a,b] O.A. Grishina,[a] O.A. Inozemtseva,[a] A.V. Selifonov,[a] D.N. Bratashov,[a] S.G. Suchkov,[a] L.A. Bulavin,[b] O.E. Glukhova,[a] G.B. Sukhorukov[c] and D.A. Gorin*[a]

Received Date
Accepted Date

DOI: 10.1039/xxxxxxxxxx

www.rsc.org/journalname

The impact of high-frequency (1.2 MHz) ultrasound with power density 0.33 W/cm$^2$ on the microcapsule nanocomposite shells with embedded zinc oxide nanoparticles was investigated by exploring modeling simulation and direct visualization. For the first time the sonication effect has been monitored *in situ* on individual microcapsules upon exposure of its aqueous suspension to ultrasound. The stress distribution on the microcapsule shell for impact of ultrasound with high (1.2 MHz) and low (20 kHz) frequency at two fixed intensities (0.33 and 30 W/cm$^2$) has been modeled. As shown *in silico* and experimentally the nanocomposite microcapsules were destroyed more effectively by action of high-frequency (1.2 MHz) ultrasound in comparison with low frequency (20 kHz) one with the same power density.

## Introduction

The development of drug delivery systems (DDS) with sensitivity to external stimuli has both potential applications in biomedical fields as well as fundamental importance in materials science [1–5]. The modern DDS require responsiveness to external impacts of different nature. The main problems of DDS development are: drug loading or incorporation in DDS structure, study of DDS biodistribution after different type of injection (intravascular, intramuscular, in skin), DDS immobilization in required place or controlled motion (passive and active targeting), the problem of barriers crossing inside the body (for example Blood-Brain Barrier) and controlled release of drug in response to external actions of physical, chemical or even biological nature. Also development of modern DDS requires some labeling to monitor its distribution inside the body. All these problems demand combination of different active components inside the single DDS. The one of well developed approaches to achieve such combination is based on L-b-L assembly of oppositely charged polyelectrolyte molecules or nanoparticles on the microparticle surface with following dissolution of template microparticle [6–9]. It allows incorporation of different structural and active materials inside the single composite capsule or core-shell microparticle [5].

The functionality of obtained microcapsules is defined by controlled size, shape, shell composition and thickness [10–15]. The polyelectrolyte microcapsules stand out among other DDS due to the attractive properties: biocompatibility, high stability in biological fluids, high encapsulation efficiency for the biologically active substances, the possibility of shell modification, biodegradation and surface functionalization [8,9,16–21]. However, effective local and non-invasive methods of controlled release of the microcapsule content in the defined location inside the human body are still under development. The problem of remote triggering the drug release from DDS had a number of solution developed up to now. The possible approaches are based on using optical radiation [22–24], EM fields [25], ultrasound [26–28], chemical triggering of release [29] and specific biochemical reactions [18,30]. Physical release triggering implies solving the main problem: the amplitude of physical fields inside the body should be high enough to make it possible, but the same field values should be obtained in high scattering media and be safe for surrounding tissues. So, the development of novel smart materials and DDS based on it with high sensitivity to physical impacts is the most important area of research in current drug delivery technologies. One of the most promising methods of such release is based on the use of ultrasound action [26]. Intensive growth of ultrasound applications in medicine including HIFU (high intensity focused ultrasound) paves the way for producing delivery carriers with sensitivity to ultrasound due to it's high penetration depth into the human body and possibility to focuse it precisely [31,32]. Moreover, ultrasound has been approved for many medical procedures, such as hyperthermia, enhancing dissolution of thrombi, acceleration

[a] *Saratov State University, Astrakhanskaya Street 83, 410012 Saratov, Russia*
[b] *Taras Shevchenko National University of Kyiv, Physics Faculty, Department of molecular physics, 64/13, Volodymyrska Street, Kyiv, Ukraine, 01601*
[c] *School of Engineering & Materials Science, Queen Mary University of London*
* *Corresponding author email:gorinda@mail.ru*
† Electronic Supplementary Information (ESI) available:

View Article Online
DOI: 10.1039/C5CP05465F





of the bone fractures healing, transdermal drug delivery and intracorporeal lithotripsy[33–35]. The power density and the penetration ability of HIFU are suitable to destroy the microcapsules and release the encapsulated substance.

The influence of ultrasound power and treatment time on destruction of polyelectrolyte microcapsule shells with different composition and parameters has been investigated since 2006[15,27,36–40]. It was established that the integrity and shell permeability of polyelectrolyte microcapsules depend on the duration of ultrasonic exposure, its power and frequency as well as the mechanical properties, thickness and chemical composition of the shell[39]. The mechanical properties of microcapsule shell can be changed by variation of inorganic nanoparticle volume fraction in the nanocomposite shell[41]. Different types of nanoparticles like silver[38], gold[37,40], magnetite[36] and zinc oxide[15,39] were incorporated into the shells to control its mechanical properties, change character of its interaction with ultrasound and in result to make the microcapsule more sensitive to ultrasound.

Up to now the fastest shell destruction by ultrasonic action was achieved by incorporation of ZnO nanoparticles into the composite shell[39]. However, the applied ultrasound parameters were still too far from ones currently used in therapeutic medicine[15,27,36–40]. The safety requirements of ultrasonic treatment and the potential possibility of using existing ultrasound diagnostic devices for the microcapsule shells rupture force the ultrasound parameters changing as well as microcapsule shell optimization. The modern trend is to increase ultrasound frequency from tens[36] to hundreds kHz[40] and decrease the required power from hundreds[36] to a few Watts[40], respectively.

So, the investigation of ultrasound impact with parameters as much as possible similar to ones used in ultrasonic medical devices and modeling of the ultrasound influence on mechanical properties of microcapsules are highly actual tasks for development of novel DDS based on polyelectrolyte microcapsules. Also there are no known models for prediction the microcapsule behavior under the ultrasound impact. The stress distribution in microcapsule shell under ultrasound action at different frequencies and power densities should be modeled and visualized *in silico*. It can be done by using finite element simulation. Incorporation of inorganic nanoparticles inside the polyelectrolyte shell could change the mechanical properties and character of ultrasound interaction with microcapsules (acoustic impedance) and as result its sensitivity to ultrasonic action can be varied[41]. The main problem with it that we cannot directly measure the ultrasound effects on the shells, but only estimate object's sensitivity to the ultrasound by time of impact and percent of capsules which saved integrity after the ultrasonic treatment. Some model should be proposed and tested on the real destruction cases to evaluate the details of this process and to investigate how the properties of microcapsule shells and ultrasound parameters influence on the microcapsule destruction. Also such model should allow comparison of results obtained with different ultrasound parameters and with different shell materials by decomposition of complex process of ultrasonic treatment into more simple dependencies.

The aim of this work is to establish the mechanical model of ultrasonic action on composite microcapsules and to predict results of ultrasound treatment for capsules with different shell composition prepared using layer-by-layer approach. The proposed simulation allows to test influence of the shell thickness and ultrasound parameters variation on sensitivity of capsules to ultrasound action. To prove the simulation correctness the optimized capsules with structure based on the model predictions should be made and tested for ultrasound sensitivity. For this goal we choose microcapsule design containing ZnO nanoparticles that was proposed in work[39] as one of the best reported up to now. We also try to visualize the impact of ultrasound on microcapsule shell *in situ* and compare the results with our simulations.

# 1 Experimental Details

## 1.1 Materials

Poly(sodium styrene sulfonate) (PSS) (MW ~70 kDa), poly(allylamine hydrochloride) (PAH) (MW ~70 kDa), sodium chloride (NaCl), tetrahydrofuran, and ZnO nanopowder (6% Al doped, less than 50 nm in size) were used without further purification and purchased from Sigma Aldrich GmbH, Germany. Monodisperse polystyrene cores with an average diameter of $10.25 \pm 0.09$ $\mu$m were purchased from Microparticles GmbH, Germany. The water used in all experiments was prepared in a three-stage Millipore Milli-Q Plus 185 purification system and had a resistivity higher than 18.2 MΩ·cm.

## 1.2 Simulation of ultrasound influence on microcapsule shells

The finite element method[42] implemented in the program complex ANSYS Workbench 13[43] was used for simulation of ultrasound influence on microcapsule shell. The model of microcapsule has spherical symmetry imposed on it. Diameter of microcapsules, shell thickness and mechanical parameters were initially taken from[39]. This bootstrap set of parameters was varied to investigate, how its change will vary the deformations of microcapsule shell. Taking into account the limitations imposed by available ultrasonic setup and L-b-L technology the optimized shell structure was developed and later fabricated. The final calculation uses the AFM measured parameters for the experimentally obtained structures and the ultrasonic setup developed to investigate impact of high frequency ultrasound on microcapsules. The calculation was done using hexahedral mesh with the maximum size of elements no more than 30 nm. It should improve the numerical convergence and minimize the influence of data sampling and grid topology on obtained strain fields and deformations (Fig. 1 a, b, c). The microcapsule shell model included in average 102 000 elements. The radial dimension of the model corresponding to the shell thickness consisted of at least three finite elements.

We assume the material properties of the shell to be linear and isotropic. The values of the effective density and Young's modulus of the shell were taken from prior work[39] for similar polyelectrolyte and nanocomposite microcapsules. For polyelectrolyte capsules density was 1100 kg/m$^3$ and elastic modulus 580 MPa, for composite capsules with three layers of ZnO it was 4482.5 kg/m$^3$ and 27.1 MPa, correspondingly. The inter-

View Article Online
DOI: 10.1039/C5CP05465F



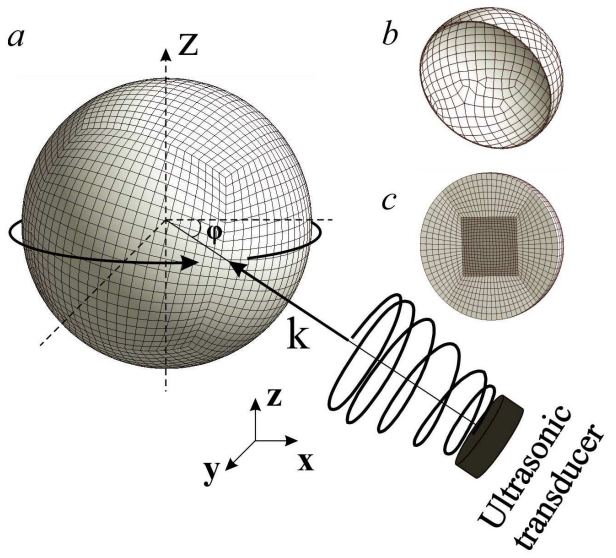


**Fig. 1** The finite element model of microcapsule shell: a — model of the ultrasound impact on the microcapsule shell, b — model grid of the microcapsule shell, c — model grid of the inner cavity of shell ($k$ — vector of acoustic pressure applied, $Z$ — the axis of microcapsule rotation, $\phi$ — the angle of microcapsule rotation)

nal volume of the capsule was considered to be filled with water. Modeled microcapsules were placed into water at temperature of $37 \pm 0.5$ °C (that corresponds to the value in the experiment).

Young modulus of polymer composite in this range of temperatures should grow slowly proportional to logarithm of frequency[44], but the change should be within error of its experimental measurement by AFM[45]. So we considered this dependence negligible in our case.

The harmonic analysis was carried out for simulation of the microcapsule shell behavior under the influence of acoustic wave with defined power density. The amplitude of the ultrasonic wave was determined by the equation:

$$I = \frac{p^2}{Z_s} \quad (1)$$

where $Z_s$ — acoustic impedance of aqueous medium, $I$ — power of ultrasound wave (W/cm$^2$). The obtained acoustic pressure amplitude $p$ was equal to 70 kPa by substitution of $I = 0.33$ W/cm$^2$ in equation (1) and 0.67 MPa for intensity equal 30 W/cm$^2$.

Frequency dependence in the model was introduced as external driving force in form of harmonic normal pressure change exerted by water on the capsule shell. The intensity of ultrasound in experiment was recalculated for finite element modeling into amplitude of water pressure change by equation (1) using the acoustic impedance of the water media $Z_s$. The frequency in our simulation was the same as in experiment. We can consider capsule shell as a kind of mass-on-spring with high damping due to water media, so we expect resonant response to external driving force with wide resonance curve. Resonant frequency for our composite capsules calculated from finite element modeling simulation was in MHz range. So we selected experimental frequency to be slightly lower than the calculated resonant eigenfrequency of the shell, but within width of resonant curve.

Linear mechanical model was used as a mathematical model for determining the microcapsule shell response to the harmonic load. This model quite well describes the real mechanical system used in our experiment. The simplification has a negligible effect on its behavior due to the fact that the external impacts on our system cause a small deformations of the microcapsule shell. This approach also was used to investigate strained-deformed state of microcapsules during its pass through the elastic microchannel[46]. It was shown that linear model behavior was in good agreement with the experimental data. The limitation of linear model is its nonapplicability to the direct simulation of the destruction process.

### 1.3 Microcapsule preparation

An alternating adsorption of oppositely charged polyelectrolytes and/or nanoparticles onto the surface of the polystyrene template particles was used for polyelectrolyte and nanocomposite microcapsule fabrication, respectively (see Supporting Information Fig. S1). For adsorption we used aqueous solutions of PAH and PSS with concentration of 2 mg/ml in the presence of 0.5 M NaCl. The adsorption time was 10 min per layer. After each deposition step the core suspension was sedimented by centrifugation and triply washed with deionized water. In the same manner as polymer molecules, ZnO nanoparticles were adsorbed onto the polyelectrolyte shell from 1 mg/ml aqueous colloid (pretreated by ultrasound during 5 min at 200 W) instead of one or three positively charged polyelectrolyte layers. After formation of shell the polystyrene cores were dissolved in tetrahydrofuran (THF) during 24 h treatment. The formed microcapsules were triply rinsed in THF to remove the residual polystyrene and finally the hollow microcapsule shells were rinsed three times in deionized water. The microcapsules with $(PAH/PSS)_6$, $(PAH/PSS)_2(ZnO/PSS)(PAH/PSS)_3$ and $(PAH/PSS)_2(ZnO/PSS)_3(PAH/PSS)$ layer structure were obtained.

### 1.4 Characterization

The microcapsules were characterized by optical microscopy, SEM, CLSM, TEM and AFM techniques. ZnO nanoparticles were also characterized by DLS methods. Measurement of the hydrodynamic size distribution for ZnO nanoparticles was performed by dynamic light scattering (DLS) at 25°C with Zetasizer Nano ZS (Malvern Ins. Ltd). The result represents the average of ten subsequent runs.

The $\zeta$-potential of the ZnO nanoparticles in aqueous solutions was also measured with Zetasizer Nano ZS (Malvern Ins. Ltd). The Smoluchowski approximation was used to convert the electrophoretic mobility to $\zeta$-potential. SEM images were obtained with Tescan Mira scanning electron microscope. Drop of the sample suspension was put onto the small silicon substrate and dried. Images of composite microcapsules were taken with 30 kV acceleration voltage using sample as is, the images of polyelectrolyte capsules were taken with 20 kV voltage using sputtering

View Article Online
DOI: 10.1039/C5CP05465F



of thin layer of gold over sample to make it conductive. TEM images were obtained using Libra-120 transmission electron microscope (Carl Zeiss, Germany) operating at 120 kV. The samples were prepared by deposition of an aqueous suspension of capsules onto the Formvar film supported by the copper grid. AFM images of microcapsules were obtained with Ntegra Spectra microscope (NT-MDT, Russia) in tapping mode. For image acquisition NSG10 probes from NT-MDT with typical resonant frequency around 220 kHz and tip curvature below 10 nm were used. The samples were prepared by drying a drop of the microcapsules aqueous suspension onto the surface of a coverglass slide. All subsequent image processing was done with Gwyddion software[47].

### 1.5 Ultrasound exposure

An ultrasonic cell was constructed for investigation of the ultrasound influence on the fabricated composite microcapsules containing ZnO nanoparticles in the shell structure as well as polyelectrolyte ones used as control (Figure 2).

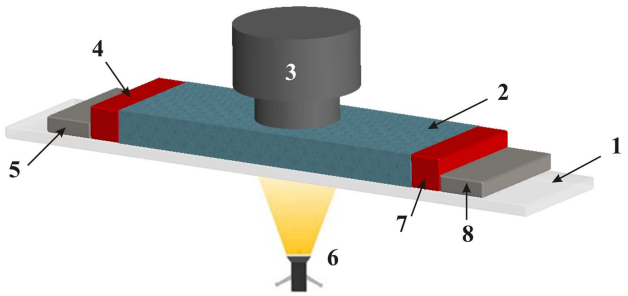


**Fig. 2** Experimental setup for ultrasound treatment of microcapsules: 1 — microscope slide, 2 — bath for an aqueous suspension of microcapsules, 3 — microscope objective, 4 — ultrasonic transducer, 5 — high-frequency-connector for transmitting the signal from oscillator, 6 — light source, 7 — reference ultrasonic transducer, 8 — high-frequency-connector to an oscilloscope for signal's frequency and power monitoring

Ultrasonic cell consisted of the piezoceramic ultrasonic transducer (4) in acoustical contact with the bath for suspension of microcapsules (2) on a microscope slide (1). Ultrasonic generator IL10 ("Ultrasonic technique — INLAB", Russia) was used for ultrasound excitation. The ultrasound with frequency of 1.2 MHz was used in our experiment. Reference transducer (7) was placed onto the glass slide to measure the obtained ultrasonic intensity in the aqueous suspension of microcapsules. The power density of ultrasound was 0.33 W/cm$^2$ which is an allowed value for diagnostic applications. To observe ultrasound effect on microcapsule shells microscope objective was immersed into the bath with microcapsules suspension. Images were captured by video camera attached to the microscope external port.

## 2 Results and Discussion

We employed a finite elements mechanical model to test influence of the shell thickness and ultrasound parameters variation on sensitivity of capsules to ultrasound action. The calculated distribution of deformation on the microcapsule surface at different ultrasound power densities and frequencies for microcapsules with shell of different thickness is shown on Fig. 3. Numerical simulations demonstrated decrease of equivalent stresses and strains arising in the microcapsule shell with higher thickness for both polyelectrolyte and nanocomposite microcapsules (Fig. 3). It was found that in the case of THF as template solvent nanocomposite microcapsules with three layers of ZnO particles were subjected to lower stress and less deformation under similar ultrasonic action. Exposure of the microcapsules to the ultrasound with frequency of 20 kHz and power density of 30 W/cm$^2$ causes the amplitude of deformation to be equal to 68 nm and 270 nm for microcapsules prepared with THF and DMF, respectively (Fig. 3 f, h). The similar trend was observed in the behavior of nanocomposite microcapsules with one ZnO layer.

Timescale for simulation of ultrasonic impact on the shell was 2 seconds that corresponds to two cycle's assessment of stress-strain state of the shell. During the first cycle strains and stresses in the initial moment of impact on the shell were calculated. The second cycle of calculation allowed us to estimate the relative growth of shell fatigue.

Fig. 3 (a, b) shows that the polyelectrolyte microcapsules (without ZnO nanoparticles) were insensitive to the ultrasound treatment with both low and high frequency at given power density. In this case the maximum deformation of the shell for capsules obtained by THF treatment was less than 80 nm and equivalent stresses were distributed homogeneously over the shell surface (the difference between the maximum and minimum stress is not exceeding 1.6 MPa). The maximum equivalent stress was 6.2 MPa.

The microcapsules in our simulation were intact at the time moment corresponding to 1 sec of ultrasonic treatment. This result is in good agreement with our experimental data as well as previously reported experiments[15,39]. Simulation of ultrasound impact on nanocomposite microcapsules $(PAH/PSS)_2(ZnO/PSS)_3(PAH/PSS)$ obtained with THF treatment, demonstrated that microcapsules were less sensitive to the effects of ultrasound at low frequency. For example, sonication at low frequency and power density causes nonsignificant deformation (the maximum amplitude of shell vibrations was less than 40 nm) that is shown in Figure 3 e. The increasing of the ultrasound power density led to the obvious increase of the shell deformation (the maximum amplitude of shell vibrations was 326 nm) (Fig. 3 f).

The model for high frequency and lower power US treatment demonstrated maximum of shell deformation to be equal 750 nm (Figure 3 j), that is similar to results for low frequency US with power density 30 W/cm$^2$. Such cyclical impact can alter through shell diffusion parameters and cause shell destruction with certain chances. The non-uniform distribution of the equivalent stresses in the shell of nanocomposite microcapsule (maximum stress was 80 MPa) appeared with increasing the power density of ultrasound treatment at 1.2 MHz. This should lead to the destruction of the nanocomposite microcapsule in 1 sec time. The simulation data were in agreement with experimental demonstration of capsule shell destruction. Also similar results were already obtained for biological cells in water media under ultrasonic action modeled using analytical approaches[48,49].

View Article Online
DOI: 10.1039/C5CP05465F



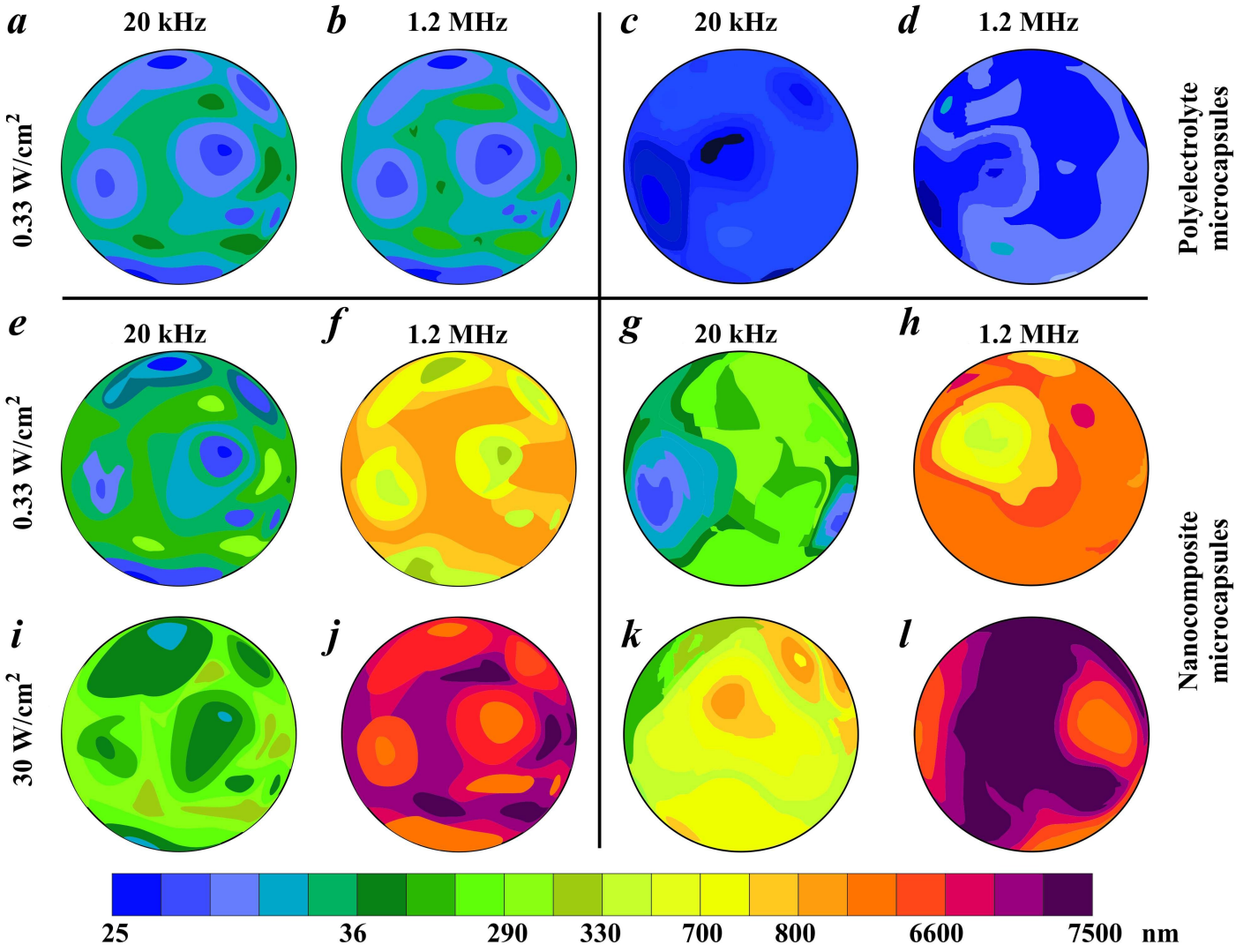


**Fig. 3** The deformation distribution in polyelectrolyte microcapsule shells with thickness 17 nm (a, b) and 32 nm (c, d) under the influence of low (20 kHz) and high frequency (1.2 MHz) ultrasound at power density 0.33 W/cm$^2$. The deformation distribution for nanocomposite microcapsule shells with thickness 256 nm (e, f, i, j) and 97 nm (g, h, k, l) under ultrasound influence with given parameters

View Article Online
DOI: 10.1039/C5CP05465F



Using the simulation we established that the ultrasound frequency of 20 kHz caused strong deformation of the shell surface. But in this case the microcapsule shell had time to relax and as the result the equivalent stresses were distributed more or less uniformly without the shell integrity damage. The high frequency ultrasound action caused high values of stresses in the nonrelaxing microcapsule shell resulting in destruction of the capsule.

The shell of microcapsule in our model has uniform thickness and homogeneous distribution of zinc oxide nanoparticles in the polymer matrix. In general, it is not always so. Different types of defects can be considered. The first one is local decreasing of shell thickness. The thinner patch of the capsule shell should have higher oscillation amplitude under ultrasonic action with the similar parameters. The second type of defects is local fluctuation of density in the microcapsules shell as result of nonhomogeneous distribution of zinc oxide nanoparticles that form aggregates. The local fluctuation of density in the microcapsules shell should change force applied to its surroundings. Any weak spot will be torn by ultrasound pressure variation earlier than uniform capsule wall. So, the developed finite element model shows upper limit for intensity required to open the capsule. Obtained non-uniform capsules should have higher sensitivity to ultrasound action in comparison with the model based on assumptions of uniform thickness and homogeneous distribution of zinc oxide nanoparticles in the polymer matrix of microcapsule shell.

To prove the simulation correctness the optimized capsules with structure based on the model predictions were fabricated by layer-by-layer assembly approach and tested for ultrasound sensitivity. ZnO nanoparticle suspension in water (with 1 mg/ml concentration and pH 7.7, pretreated with ultrasound during 1 min at 200 W power) was used to produce the nanocomposite microcapsule shells. The mean hydrodynamic size of ZnO nanoparticles was about $130 \pm 60$ nm (PDI 0.44) and $\zeta$-potential was $28 \pm 6$ mV at given pH (see Supporting Information, Fig. S2 a, b). ZnO nanoparticles were incorporated into the microcapsule shell instead of the one or three positively charged poly(allylamine hydrochloride) (PAH) layers in the middle of layer structure resulting in $(PAH/PSS)_2(ZnO/PSS)(PAH/PSS)_3$ and $(PAH/PSS)_2(ZnO/PSS)_3(PAH/PSS)$.

SEM images of microcapsules at different magnifications with and without ZnO nanoparticles are presented in Fig. 4 (a, b, c) and Fig. 4 (d, e, f), respectively. SEM images of nanocomposite and pure polymer microcapsules showed that the microcapsules were collapsed after drying. Dried microcapsules showed some diameter shrinking and were not strongly aggregated (Fig. 4 (a, b)).

Composite capsules (Fig. 4 b, c) are more inhomogeneous in surface morphology with inclusions up to hundred nanometers in size in comparison with smooth surface of pure polyelectrolyte microcapsule (Fig. 4 e, f). The SEM data (Fig. 3 b, e) are confirmed by TEM investigation (Fig. 5 a, b).

The TEM images of composite microcapsule (Fig. 5 a, b) show that the ZnO nanoparticles tended to form large non-spherical irregular shaped aggregates in the microcapsule shell up to hundred nanometers in size with high density packing. The average size of ZnO nanoparticle aggregates measured by TEM

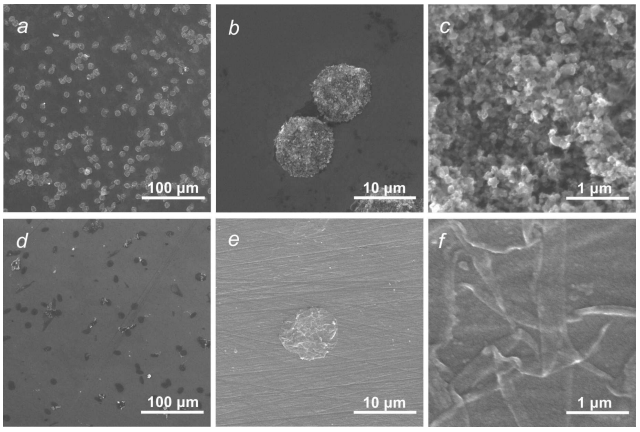


**Fig. 4** SEM images of nanocomposite microcapsules with $(PAH/PSS)_2(ZnO/PSS)_3(PAH/PSS)$ layer structure (a, b, c) at different magnifications and polyelectrolyte microcapsules with $(PAH/PSS)_6$ layer structure (d, e, f)

(Fig. 5 c, d) is similar to that of initial colloid measured by DLS. The value in the both cases is higher than reported in[39] despite the fact that we used the same ZnO nanoparticles from the same supplier. This can be caused by lower ultrasound power during ZnO pretreatment in our experiment.

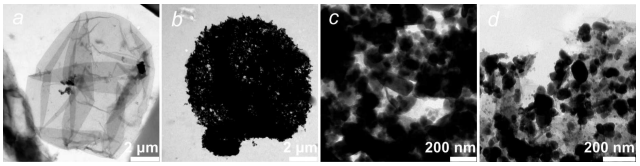


**Fig. 5** TEM images of polyelectrolyte microcapsule with $(PAH/PSS)_6$ layer structure (a), nanocomposite microcapsule with $(PAH/PSS)_2(ZnO/PSS)_3(PAH/PSS)$ layer structure (b, c) at different magnifications and ZnO nanoparticles (d) used for microcapsule shell fabrication

The AFM method was used for the quantititive characterization of microcapsules morphological parameters such as the average shell thickness, the effective thickness of one ZnO nanoparticle layer, the average shell roughness ($R_a$) and the size of ZnO aggregates in composite shell after drying (Fig. 6). At least three different capsules were measured from each sample and the data were averaged. For the parameter estimation imaging artifacts were removed, base plane of the substrate was subtracted and flattened as much as possible with methods available in Gwyddion data processing software. Diameter for flattened dried capsule was evaluated by selecting the whole capsule as grain, measuring its projected surface area and recalculate it to the equivalent disk diameter. The shell roughnes was measured as $R_a$ value for relatively flat parts of the collapsed shell double layer similar to[15]. Shell thickness was determined by evaluating height distribution for the same flattened areas, measuring the peak maximum position and substracting the average height of substrate background (the maximum position of the first peak on heigh distribution histogram of the whole image). The shell thickness was determined as the difference between the substrate surface and the thinnest planar part of the collapsed microcapsule. The average size of

View Article Online
DOI: 10.1039/C5CP05465F



ZnO nanoparticle aggregates from AFM measurement calculated from particles projected area in lateral dimension is about 160 nm that has a good agreement with TEM (see Fig. 5) and DLS (see Supporting Information, Fig. S2) data.

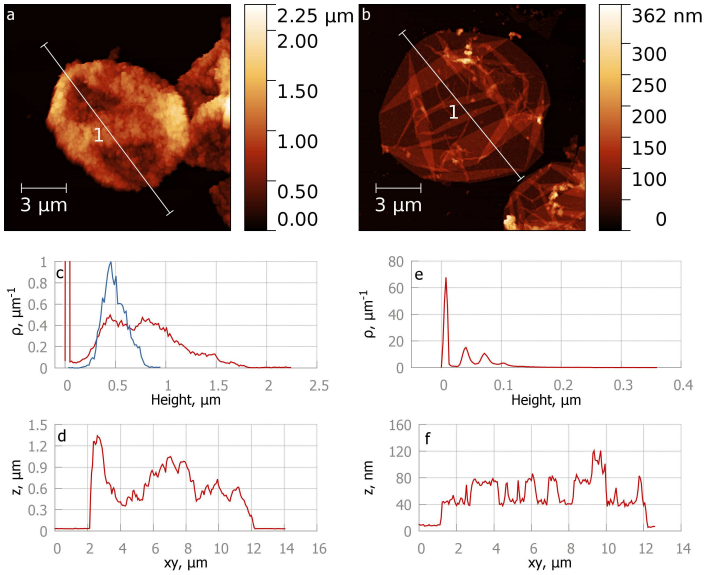


**Fig. 6** AFM height data of nanocomposite (a) and polyelectrolyte (b) microcapsules. Height distribution function for the whole image (red) and double layer part (blue, scaled ×0.25) (c) and height profile along line 1 (d); Height distribution function (e) and profile along line 1 for polyelectrolyte microcapsule (f)

AFM data show that the average shell thickness for the collapsed polyelectrolyte microcapsule was two times less than reported before[39], 17 and 32 nm, correspondingly (see Table 1). This can be explained by strong dehydration of polyelectrolyte layer as the result of core dissolution by THF in comparison with DMF. Nevertheless, the average shell thickness for nanocomposite microcapsules was higher than previously reported value[39]. It can be caused by using different ultrasound power for ZnO colloid pretreatment that was 600 W in work[39] and 200 W in our experiment. This can provide a large difference in size distribution of nanoparticle aggregates in colloid. The hypotesis was also confirmed by effective thickness of one ZnO layer (see Table 1) calculated from AFM data. So the effective shell thickness for nanocomposite microcapsule corresponds to the average size of nanoparticle aggregates (slightly less for three ZnO layer structure probably due to packing the large particles in higher layers into concave places between underlying particles).

In the work by Kolesnikova et al.[39] some microcapsules shell diameter enlargement was observed after drying the suspension. Besides, the dried shells exhibit flattened shape without folds typical for dried microcapsules. So the composite layer in this case had high elasticity for extension. In our experiments the composite capsule shells kept its size upon drying. The characteristic thick folds were observed on the microcapsule shell with ZnO layers. Even though our experiment data cannot be directly compared with work[39] because we used larger ZnO nanoparticles and lower power for ultrasound pretreatment of ZnO nanoparticles, there are solid reasons to presume that the main differences in microcapsules shell properties are caused by using different solvents to remove the template core.

**Table 1** Influence of solvent (DMF or THF) on the average shell parameters of polyelectrolyte and nanocomposite microcapsules with the following shell structures:
A) $(PAH/PSS)_6$; B) $(PAH/PSS)_2(ZnO/PSS)(PAH/PSS)_3$;
C) $(PAH/PSS)_2(ZnO/PSS)_3(PAH/PSS)$. The values in brackets corresponds to polyelectrolyte layer thickness

| Solvent | DMF[39] | | | THF | | |
|---|---|---|---|---|---|---|
| Shell Structures | A | B | C | A | B | C |
| Average shell thickness (nm) | 32 | 38 | 97 | 17 | 116 | 256 |
| Average roughness $R_a$ (nm) | 8.6 | 43 | 25 | 4.6 | 59 | 116 |
| Average shell diameter ($\mu$m) | 10.2 | 11.1 | 13.1 | 11.0 | 9.9 | 9.0 |
| Effective thickness of one ZnO layer (nm) | (2.7) | 8.2 | 24.2 | (1.4) | 100.6 | 81.1 |

Due to thicker microcapsule shell we expect slightly lower sensitivity of our nanocomposite microcapsules to impact of low frequency ultrasound as was shown by the model described above.

After characterization of microcapsules the effect of ultrasound with frequency of 1.2 MHz and power density of 0.33 W/cm$^2$ on the nanocomposite microcapsules dispersed in water was studied with developed setup (see Fig. 2). The applied ultrasound power density was below cavitation threshold for liquids and biological tissues[33–35,50].

Simulation and *in situ* video recording demonstrated the rotation of microcapsules around the *Z*-axis under the influence of ultrasound with wave vector along the *k*-direction shown on Fig. 2 a. The purple gradient background on the Fig. 7 a indicates the stabilization time for numerical model. Green gradient corresponds to the simulation of the microcapsule behavior with stable numerical model and optical microscopy visualization. The capsule rotation can be explained by the interaction of the ultrasonic wave and the shell shape changes under the influence of intrinsic vibrational eigenmodes at different time moments. The result of visualized ultrasound treatment showed that about 75% of the microcapsules were destroyed by sonication during the first 3 seconds of impact (Figure 7 b, c). Thus, we have shown that the polyelectrolyte microcapsules with embedded ZnO nanoparticles (nanocomposite microcapsules) can be destroyed by ultrasound with frequency of 1.2 MHz and power density of 0.33 W/cm$^2$ that allows using the similar microcapsules as potential DDS with controlled release.

## 3 Conclusions

For the first time linear mechanical model of microcapsules for visualization of the deformation and stress distributions in the microcapsule shells with different composition and thickness under impact of ultrasound with different parameters was proposed. Simulations demonstrated that the increase of ultrasound power and its frequency leads to increase of the equivalent stress on the shell surface that can cause microcapsule destruction. Increasing the microcapsule shell thickness reduces the deformations emerging on the surface. The proposed model of microcapsules behav-

View Article Online
DOI: 10.1039/C5CP05465F



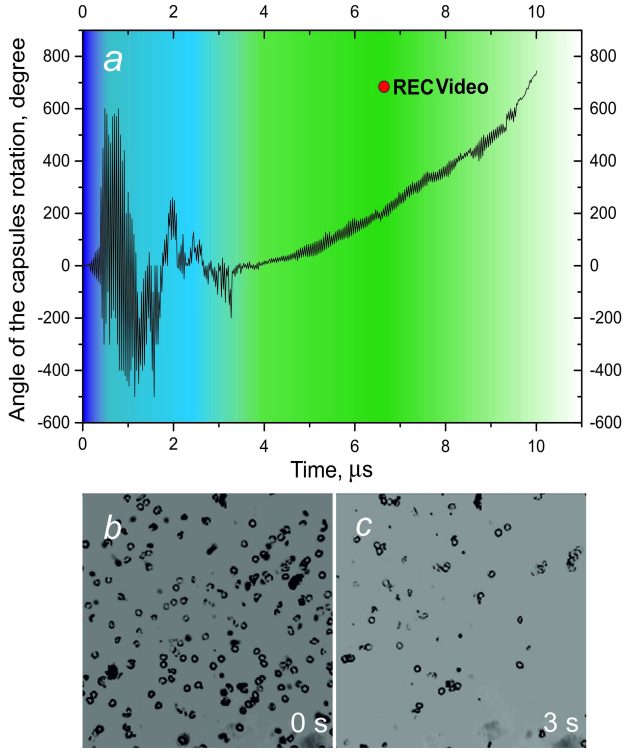


**Fig. 7** The angle of microcapsule rotation around its axis under the ultrasound influence (a). Still frames from the video recording (Supplementary Movie) of the impact of high frequency ultrasound on nanocomposite microcapsules before (b) and after 3 sec. of ultrasound exposure (c)

ior under the ultrasonic treatment allowed us to optimize microcapsule shell properties and to achieve the possibility of applying high frequency (1.2 MHz) ultrasound approved for human use at power density of 0.33 W/cm$^2$ for the destruction of nanocomposite microcapsules with three ZnO nanoparticles layers that was visualized *in situ* by optical microscopy in our experiment. It opens the way to further using of such microcapsules in DDS intented to use with HIFU setup. The DDS can be triggered to drug release in any depth inside the living system where ultrasound can be focused without damaging surrounding tissue. However, the developed model does not take into account the shape and size of the discontinuities in the capsule shell that should be considered in the future.

## 4 Acknowledgements

The authors thank Viktor Galushka for the SEM measurements and Dr. Boris Khlebtsov for the TEM measurements. This work was partly supported by Government of the Russian Federation (grant No. 14.Z50.31.0004 to support scientific research projects implemented under the supervision of leading scientists at Russian institutions and Russian institutions of higher education).

## References

1 V. P. Torchilin, *Nature Reviews Drug Discovery*, 2014, **13**, 813–827.
2 C. Alvarez-Lorenzo and A. Concheiro, *Chem. Commun.*, 2014, **50**, 7743–7765.
3 Y. Zhang, H. F. Chan and K. W. Leong, *Advanced Drug Delivery Reviews*, 2013, **65**, 104–120.
4 M. A. C. Stuart, W. T. S. Huck, J. Genzer, M. Muller, C. Ober, M. Stamm, G. B. Sukhorukov, I. Szleifer, V. V. Tsukruk, M. Urban, F. Winnik, S. Zauscher, I. Luzinov and S. Minko, *Nature Materials*, 2010, **9**, 101–113.
5 P. Wuytens, B. Parakhonskiy, A. Yashchenok, M. Winterhalter and A. Skirtach, *Current Opinion in Pharmacology*, 2014, **18**, 129–140.
6 G. Decher, *Science*, 1997, **277**, 1232–1237.
7 G. Decher and J. Hong, *Berichte der Bunsengesellschaft für physikalische Chemie*, 1991, **95**, 1430–1434.
8 W. Tong, X. Song and C. Gao, *Chemical Society Reviews*, 2012, **41**, 6103–6124.
9 K. Ariga, Y. M. Lvov, K. Kawakami, Q. Ji and J. P. Hill, *Advanced drug delivery reviews*, 2011, **63**, 762–771.
10 T. A. Kolesnikova, A. G. Skirtach and H. Möhwald, *Expert opinion on drug delivery*, 2013, **10**, 47–58.
11 D. V. Volodkin, S. Schmidt, P. Fernandes, N. I. Larionova, G. B. Sukhorukov, C. Duschl, H. Möhwald and R. von Klitzing, *Advanced Functional Materials*, 2012, **22**, 1914–1922.
12 F. Zhang, Q. Wu, L.-J. Liu, Z.-C. Chen and X.-F. Lin, *International journal of pharmaceutics*, 2008, **357**, 22–31.
13 C. Gao, S. Leporatti, S. Moya, E. Donath and H. Möhwald, *Chemistry-A European Journal*, 2003, **9**, 915–920.
14 A. A. Antipov, G. B. Sukhorukov, S. Leporatti, I. L. Radtchenko, E. Donath and H. Möhwald, *Colloids and Surfaces A: Physicochemical and Engineering Aspects*, 2002, **198**, 535–541.
15 T. Kolesnikova, B. Khlebtsov, D. Shchukin and D. Gorin, *Nanotechnologies in Russia*, 2008, **3**, 560–569.
16 W. Tong and C. Gao, *Journal of Materials Chemistry*, 2008, **18**, 3799–3812.
17 G. B. Sukhorukov, A. L. Rogach, M. Garstka, S. Springer, W. J. Parak, A. Muñoz-Javier, O. Kreft, A. G. Skirtach, A. S. Susha, Y. Ramaye *et al.*, *Small*, 2007, **3**, 944–955.
18 B. De Geest, R. Vandenbroucke, A. Guenther, G. Sukhorukov, W. Hennink, N. Sanders, J. Demeester and S. De Smedt, *Advanced Materials*, 2006, **18**, 1005–1009.
19 D. B. Shenoy, A. A. Antipov, G. B. Sukhorukov and H. Möhwald, *Biomacromolecules*, 2003, **4**, 265–272.
20 A. G. Skirtach, A. M. Yashchenok and H. Möhwald, *Chemical Communications*, 2011, **47**, 12736–12746.
21 B. G. De Geest, S. De Koker, G. B. Sukhorukov, O. Kreft, W. J. Parak, A. G. Skirtach, J. Demeester, S. C. De Smedt and W. E. Hennink, *Soft Matter*, 2009, **5**, 282–291.
22 Y. Wu, J. Frueh, T. Si, H. Mohwald and Q. He, *Phys. Chem. Chem. Phys.*, 2015, **17**, 3281–3286.
23 Q. Yi and G. B. Sukhorukov, *Advances in Colloid and Interface Science*, 2014, **207**, 280–289.
24 D. A. Gorin, S. A. Portnov, O. A. Inozemtseva, Z. Luklinska, A. M. Yashchenok, A. M. Pavlov, A. G. Skirtach, H. Möhwald and G. B. Sukhorukov, *Physical Chemistry Chemical Physics*, 2008, **10**, 6899–6905.

View Article Online
DOI: 10.1039/C5CP05465F



25 N. L. Klyachko, M. Sokolsky-Papkov, N. Pothayee, M. V. Efremova, D. A. Gulin, N. Pothayee, A. A. Kuznetsov, A. G. Majouga, J. S. Riffle, Y. I. Golovin and A. V. Kabanov, *Angewandte Chemie*, 2012, **124**, 12182–12185.

26 W. G. Pitt, G. A. Husseini and B. J. Staples, *Expert opinion on drug delivery*, 2004, **1**, 37–56.

27 H. Gao, D. Wen and G. B. Sukhorukov, *J. Mater. Chem. B*, 2015, **3**, 1888–1897.

28 N. Huebsch, C. J. Kearney, X. Zhao, J. Kim, C. A. Cezar, Z. Suo and D. J. Mooney, *Proceedings of the National Academy of Sciences*, 2014, **111**, 9762–9767.

29 Y. Ma, W.-F. Dong, M. A. Hempenius, H. Möhwald and G. J. Vancso, *Nature materials*, 2006, **5**, 724–729.

30 M. V. Lomova, A. I. Brichkina, M. V. Kiryukhin, E. N. Vasina, A. M. Pavlov, D. A. Gorin, G. B. Sukhorukov and M. N. Antipina, *ACS Applied Materials & Interfaces*, 2015, **7**, 11732–11740.

31 N. Hijnen, S. Langereis and H. Grüll, *Advanced drug delivery reviews*, 2014, **72**, 65–81.

32 C. Lovegrove, *Nature Clinical Practice Oncology*, 2006, **3**, 8–9.

33 D. L. Miller, N. B. Smith, M. R. Bailey, G. J. Czarnota, K. Hynynen, I. R. S. Makin *et al.*, *Journal of Ultrasound in Medicine*, 2012, **31**, 623–634.

34 I. Lentacker, I. De Cock, R. Deckers, S. De Smedt and C. Moonen, *Advanced drug delivery reviews*, 2014, **72**, 49–64.

35 S. B. Barnett, G. R. Ter Haar, M. C. Ziskin, H.-D. Rott, F. A. Duck and K. Maeda, *Ultrasound in medicine & biology*, 2000, **26**, 355–366.

36 D. G. Shchukin, D. A. Gorin and H. Möhwald, *Langmuir*, 2006, **22**, 7400–7404.

37 B. G. De Geest, A. G. Skirtach, A. A. Mamedov, A. A. Antipov, N. A. Kotov, S. C. De Smedt and G. B. Sukhorukov, *Small*, 2007, **3**, 804–808.

38 A. G. Skirtach, B. G. De Geest, A. Mamedov, A. A. Antipov, N. A. Kotov and G. B. Sukhorukov, *Journal of materials chemistry*, 2007, **17**, 1050–1054.

39 T. A. Kolesnikova, D. A. Gorin, P. Fernandes, S. Kessel, G. B. Khomutov, A. Fery, D. G. Shchukin and H. Möhwald, *Advanced Functional Materials*, 2010, **20**, 1189–1195.

40 A. M. Pavlov, V. Saez, A. Cobley, J. Graves, G. B. Sukhorukov and T. J. Mason, *Soft Matter*, 2011, **7**, 4341–4347.

41 M. F. Bédard, A. Munoz-Javier, R. Mueller, P. Del Pino, A. Fery, W. J. Parak, A. G. Skirtach and G. B. Sukhorukov, *Soft Matter*, 2009, **5**, 148–155.

42 T. J. Hughes, *The finite element method: linear static and dynamic finite element analysis*, Courier Corporation, 2012.

43 H.-H. Lee, *Finite element simulations with ANSYS Workbench 14*, SDC publications, 2012.

44 N. Lagakos, J. Jarzynski, J. H. Cole and J. A. Bucaro, *Journal of Applied Physics*, 1986, **59**, 4017–4031.

45 P. Schön, K. Bagdi, K. Molnár, P. Markus, B. Pukánszky and G. J. Vancso, *European Polymer Journal*, 2011, **47**, 692–698.

46 G. Zhu, A. Alexeev and A. C. Balazs, *Macromolecules*, 2007, **40**, 5176–5181.

47 D. Nečas and P. Klapetek, *Central European Journal of Physics*, 2012, **10**, 181–188.

48 P. V. Zinin, J. S. Allen and V. M. Levin, *Phys. Rev. E*, 2005, **72**, 061907.

49 P. V. Zinin and J. S. Allen, *Phys. Rev. E*, 2009, **79**, 021910.

50 J.-L. Capelo-Martínez, *Ultrasound in chemistry: analytical applications*, John Wiley & Sons, 2008.